Pro-Inflammatory CD11c$^+$CD206$^+$ Adipose Tissue Macrophages Are Associated With Insulin Resistance in Human Obesity

John M. Wentworth,[1,2,3] Gaetano Naselli,[1] Wendy A. Brown,[3] Lisa Doyle,[3] Belinda Phipson,[4] Gordon K. Smyth,[4] Martin Wabitsch,[5] Paul E. O'Brien,[3] and Leonard C. Harrison[1,2]

OBJECTIVE—Insulin resistance and other features of the metabolic syndrome have been causally linked to adipose tissue macrophages (ATMs) in mice with diet-induced obesity. We aimed to characterize macrophage phenotype and function in human subcutaneous and omental adipose tissue in relation to insulin resistance in obesity.

RESEARCH DESIGN AND METHODS—Adipose tissue was obtained from lean and obese women undergoing bariatric surgery. Metabolic markers were measured in fasting serum and ATMs characterized by immunohistology, flow cytometry, and tissue culture studies.

RESULTS—ATMs comprised CD11c$^+$CD206$^+$ cells in "crown" aggregates and solitary CD11c$^-$CD206$^+$ cells at adipocyte junctions. In obese women, CD11c$^+$ ATM density was greater in subcutaneous than omental adipose tissue and correlated with markers of insulin resistance. CD11c$^+$ ATMs were distinguished by high expression of integrins and antigen presentation molecules; interleukin (IL)-1β, -6, -8, and -10; tumor necrosis factor-α; and CC chemokine ligand-3, indicative of an activated, proinflammatory state. In addition, CD11c$^+$ ATMs were enriched for mitochondria and for RNA transcripts encoding mitochondrial, proteasomal, and lysosomal proteins, fatty acid metabolism enzymes, and T-cell chemoattractants, whereas CD11c$^-$ ATMs were enriched for transcripts involved in tissue maintenance and repair. Tissue culture medium conditioned by CD11c$^+$ ATMs, but not CD11c$^-$ ATMs or other stromovascular cells, impaired insulin-stimulated glucose uptake by human adipocytes.

CONCLUSIONS—These findings identify proinflammatory CD11c$^+$ ATMs as markers of insulin resistance in human obesity. In addition, the machinery of CD11c$^+$ ATMs indicates they metabolize lipid and may initiate adaptive immune responses.
Diabetes **59:1648–1656, 2010**

The metabolic syndrome associated with obesity is characterized by insulin resistance, hyperglycemia, hypertension, and dyslipidemia, reversible by weight loss (1). Studies in obese mice indicate that adipose tissue inflammation, centered on macrophages recruited to and activated by an expanding adipose tissue mass, is a mechanistic link between obesity and insulin resistance. The density of adipose tissue macrophages (ATMs) correlates with adipose tissue inflammatory markers and insulin resistance (2), but, more importantly, mice that lack the proinflammatory enzyme IκB kinase-β in macrophages do not develop diet-induced insulin resistance (3), and mice that lack the anti-inflammatory transcription factor peroxisome proliferator–activated receptor-γ in macrophages develop insulin resistance (4,5).

Two ATM populations have been described in mice. In lean animals, solitary "resident" ATMs predominate. These ATMs have an "alternative" (M2) macrophage phenotype characterized by increased expression of interleukin (IL)-10 and arginase (6) and may facilitate adipogenesis (7). Obese mice also exhibit "crown" macrophages aggregated around necrotic adipocytes (8). These ATMs have increased expression of the integrin CD11c and markers of "classical" (M1) macrophages, including IL-6 and inducible nitric oxide (NO) synthase (6,9,10). The phenotypic switch from M2 to M1 could be an important determinant of insulin resistance in obese mice because CD11c promoter–dependent conditional deletion of ATMs improves insulin sensitivity (11).

A role for ATMs in the pathophysiology of human insulin resistance is less well established. As in mice, adipose tissue of obese humans exhibits increased expression of genes encoding proinflammatory cytokines (12) and contains increased numbers of ATMs compared with adipose tissue from lean control subjects (13,14). However, ATM density, determined by histology or CD68 mRNA expression, was found to correlate weakly or not at all with insulin resistance (15–17). In addition, the existence of M1 and M2 ATM subsets has not been confirmed. A role for ATMs in human insulin resistance is also confounded by several differences between mice and humans. These include increased expression of resistin (18) and reduced expression of inducible NO synthase (19) and arginase (20) in human macrophages and reduced expression of CD11c by ATMs (21) and a relative paucity of crown macrophages in human adipose tissue (17,21,22). To better understand the role of ATMs in human obesity and insulin resistance, we enumerated and characterized ATMs from lean and obese women.

From the [1]Autoimmunity and Transplantation Division, Walter and Eliza Hall Institute of Medical Research, Victoria, Australia; the [2]Burnet Clinical Research Unit, Royal Melbourne Hospital, Victoria, Australia; the [3]Centre for Obesity Research and Education, Monash University, Commercial Road, Victoria, Australia; the [4]Bioinformatics Division, Walter and Eliza Hall Institute of Medical Research, Victoria, Australia; and the [5]Department of Pediatrics and Adolescent Medicine, University of Ulm, Ulm, Germany.
Corresponding author: Leonard C. Harrison, harrison@wehi.edu.au.
Received 3 March 2009 and accepted 15 March 2010. Published ahead of print at http://diabetes.diabetesjournals.org on 31 March 2010. DOI: 10.2337/db09-0287.

RESEARCH DESIGN AND METHODS

Subjects and tissue. Initially, tissues were obtained from 29 Caucasian women undergoing laparoscopic surgery for insertion or revision of a gastric band. Subsequently, tissues were obtained from a further 89 Caucasian women to confirm initial findings and undertake mechanistic studies. Subcutaneous and omental adipose tissues were resected from the peri-umbilical region and omentum near the Angle of His, respectively, placed in DMEM (Sigma, Sydney, Australia) supplemented with 20 mmol/l HEPES (Sigma) and transported to the laboratory within 2 h. Approval was given by the human research and ethics committees of The Avenue Hospital and the Walter and Eliza Hall Institute of Medical Research.

Biochemistry. Analyses were performed on fasting blood samples provided within 3 months of surgery. Insulin resistance was determined using the homeostasis model assessment (HOMA) 2 calculator (46). Adiponectin and leptin Luminex assays (Linco Research, St. Charles, MO) and high–molecular weight adiponectin enzyme-linked immunosorbent assays (Fujirebio, Japan) were performed on sera collected immediately prior to anesthesia. Cytokine/chemokine concentrations in cell culture supernatants were determined by Luminex assays (Linco Research).

Immunohistochemistry. Formalin-fixed 5-μm adipose tissue sections were dewaxed in xylene and boiled in antigen-unmasking solution (Vector, Sacramento, CA) for 15 min. Frozen 12-μm sections cut from adipose tissue embedded in optimal cutting temperature (OCT) compound (Tissue-Tek, Torrance, CA) were fixed in acetone. Primary antibodies used were CD68 (PG-M1; Dako, Glostrup, Denmark), CD11c (563; Novocastra, Newcastle upon Tyne, U.K.), CD206 (551135; BD Biosciences, Lane Cove, NSW, Australia), and voltage-dependent anion channel (VDAC1) (ab14734; Abcam, Cambridge, U.K.). For single-antibody stains, sections were treated with 1% H_2O_2 then washed in PBS before overnight incubation with primary antibody. Antigen signal was detected by further incubation with biotinylated anti-mouse IgG antibody (Dako), followed by streptavidin–horseradish peroxidase (Vector) and then DAB+ liquid (DAKO). For immunofluorescence, anti-mouse Alexa 488 (Invitrogen, Carlsbad, CA), biotinylated anti-mouse IgG_3 (BD Biosciences), and streptavidin–Alexa 594 (Invitrogen) were used as secondary antibodies. Images were obtained using an Axioskop2 microscope (Zeiss, Munich, Germany) and AxioVision version 4.6 software (Zeiss). Oil red O staining was performed on cells fixed in formalin vapor by incubation in 0.6% wt/vol Oil red O (Sigma) in 60% vol/vol isopropanol for 15 min followed by counterstaining with hematoxylin.

Crowns were defined as three or more CD68-positive cells surrounding an adipocyte, and crown density was defined as the number of crowns per high-power field. A minimum of four low-power (40×) fields was counted on two separate occasions by one observer (J.W.), blinded to the adipose tissue donor. Mean adipocyte size in pixels was determined from three 100× fields using ImageJ software (National Institutes of Health, Bethesda, MD).

Adipose tissue digestion and flow cytometry. Adipose tissue was minced with sterile scissors, centrifuged at 755*g* to remove blood cells, and digested in DME/HEPES (10 ml/2 g) supplemented with 10 mg/ml fatty acid–poor BSA (Calbiochem, San Diego, CA), 35 μg/ml liberase blendzyme 3 (Roche, Indianapolis, IN), and 60 units/ml DNAse I (Sigma) in a 37° water bath. Samples were minced every 5 min for 50 min then passed through a sterile strainer before centrifuging at 612*g*. The stromovascular cell pellet was treated with red cell lysis solution (155 mmol/l NH_4Cl, 10 mmol/l $KHCO_3$, and 90 μmol/l EDTA), applied to a 70-μm filter, and suspended in fluorescence-activated cell sorting (FACS) buffer (PBS/1 mmol/l EDTA/5 mg/ml fatty acid–poor BSA). For cytokine release and gene microarray experiments, stromovascular cells were initially separated into $CD14^+$ and $CD14^-$ fractions with anti-CD14 magnetic beads and MS separation columns (Miltenyi, North Ryde, NSW, Australia).

Flow cytometry was performed on a FACSAria (weekly coefficient of variation <7%) and analyzed with FacsDiva version 6.0 software (BD Biosciences). Cells were stained in the presence of 10% vol/vol fluorochrome-conjugated antibodies and suspended in FACS buffer containing 0.05 μg/ml propidium iodide. FSc-A/FSc-H and propidium iodide gates were used to identify single, live cells. Fluorescence intensity was normalized by subtracting the fluorescence intensity of phycoerythrin (PE)-conjugated isotype control antibody or of cells incubated in the absence of Mitotracker red. For cell sorting, $CD14^+$, $CD14^-$, or stromovascular preparations were stained with CD11c-allophycocyanin, CD14–fluorescein isothiocyanate (FITC), CD45-PC7, and CD206-PE antibodies. The purity of all isolations was >90% (supplemental Fig. 2, available at http://diabetes.diabetesjournals.org/cgi/content/full/db09-0287/DC1). All antibodies were obtained from BD Biosciences, with the exception of TLR2-PE and TLR4-PE (BioLegend, San Diego, CA), CCR2-PE (R&D Systems, Minneapolis, MN), and CD14-PC7 and CD45-PC7 (Beckman Coulter, Paris, France). Mitotracker red mitochondrial dye was from Molecular Probes (Eugene, OR).

Conditioned medium. For measurement of secreted cytokines, ATMs were sorted from the $CD14^+$ stromovascular population, suspended at 20,000 in 100 μl RPMI medium (Sigma) supplemented with 10% FCS (Thermo Electron, Melbourne), and cultured ±20 ng/ml lipopolysaccharide (LPS) in 96-well flat-bottom tissue culture plates (BD Labware, Franklin Lakes, NJ) for 24 h. Cell viability after 24 h, determined by ethidium bromide/acridine orange uptake (BDH Chemicals, Poole, U.K.), was 60–90%. To condition medium to screen for inhibition of insulin action, individual cell types were sorted directly from the stromovascular population, suspended in serum-free F3 medium (DME/HAMF12 containing 8 mg/l biotin, 4 mg/l pantothenate, 2 mg/l gentamicin, 2 mmol/l Glutamax, 10 mg/l transferrin, 200 pmol/l triiodothyronine, and 100 nmol/l hydrocortisone; all from Sigma), and cultured in 96-well round-bottom plates for 48 h.

Insulin-stimulated glucose uptake. Freshly isolated human adipocytes rapidly lose viability and sensitivity to insulin. The human Simpson-Golabi-Behmel syndrome (SGBS) preadipocyte (PA) cell line, which is neither transformed nor immortalized, can be induced to differentiate in vitro, providing a unique tool for the study of human adipocytes and their response to insulin (47). SGBS PAs were first differentiated in 96-well plates as previously described (47) and then cultured for 48 h in serum-free F3 medium conditioned (20% vol/vol) by medium from total stromovascular cells, $CD11c^+CD206^+$ ATMs, $CD11c^-$ ATMs, lymphocyte (LYM), or PA cells. After 48 h, adipocyte morphology and lactate dehydrogenase (LDH) activity of the supernatant was not significantly different between groups. Adipocytes were then washed in Krebs-Ringer phosphate (KRP) buffer (136 mmol/l NaCl, 4.5 mmol/l KCL, 1.25 mmol/l $CaCl_2$, 1.25 mmol/l $MgCl_2$, 0.6 mmol/l Na_2HPO_4, 0.4 mmol/l NaH_2PO_4, 10 mmol/l HEPES, and 0.1% BSA), incubated at 37°C for 20 min in 40 μl KRP with or without insulin before addition of 10 μl KRP containing 0.25 mmol/l unlabeled 2-deoxyglucose and 0.1 μCi tritiated 2-deoxyglucose (Perkin Elmer) for a further 10 min. Cells were then washed with ice-cold PBS containing 80 mg/l phloretin (Sigma) before lysis in 0.1 mol/l NaOH, transfer into UltimaGold scintillant (Perkin Elmer), and β-scintillation counting. Counts (cpm) were corrected for cell-free blanks. The intra-assay coefficient of variation for replicate control wells was 5–18%.

Quantitative PCR and gene microarray. RNA was prepared from cell pellets using a Picopure RNA kit (Arcturus, Oxnard, CA). DNA was prepared by proteinase K digestion and ethanol precipitation. Primer sequences are shown (supplemental Table 2). Amplification efficiencies of primer pairs were not significantly different over the concentration ranges measured. For RT-PCR, total RNA was reverse transcribed using Superscript III (Invitrogen) and amplified on an ABI Prism 7700 platform using the Sybergreen reporter (Qiagen, Valencia, CA). Gene expression relative to β-actin was determined using the comparative C_T method.

Gene microarray of $CD11c^-$ and $CD11c^+CD206^-$ ATMs was performed using 50 ng total RNA and human WG-6 v2 bead chips (Illumina, San Diego, CA). Microarray analysis used the lumi, limma, and annotation packages of Bioconductor (48). Expression data were background corrected using negative control probes followed by a variance-stabilizing transformation (49) and quantile normalization. Gene-wise linear models were fitted to determine differences between cell populations, taking into account subject-to-subject variability. Significant differentially expressed genes were identified using empirical Bayes moderated *t* tests and a false discovery rate of 5% (50). Functional annotation clustering analysis (25) of differentially expressed genes was performed online (www.david.abcc.ncifcrf.gov/home.jsp) using default settings.

Statistical analysis. Statistical analyses were performed with Prism version 5.0a software for Macintosh (Graphpad, San Diego, CA). Pairs of groups were compared by the Mann-Whitney test or Wilcoxon matched-pairs test, as appropriate. Multiple groups were analyzed by ANOVA, with Newman-Keuls posttest comparisons of group pairs. Correlation was determined by Spearman rank-log test. $P < 0.05$ was considered significant.

RESULTS

Crown ATMs express CD11c. Subcutaneous and omental adipose tissue was obtained from obese women (BMI range 39–56 kg/m^2) undergoing bariatric surgery. In tissue sections stained for the monocyte/macrophage marker CD68, the majority of monocytes/macrophages appeared as slender, "resident" cells at the junctions of two or more adipocytes (Fig. 1*A*). Less frequently, ATMs surrounded adipocytes in heterogeneously distributed crown aggregates. Crown ATMs were larger, ovoid cells that occasionally coalesced to form syncytial giant cells (Fig. 1*A*). Scattered monocytes were also observed within arterioles

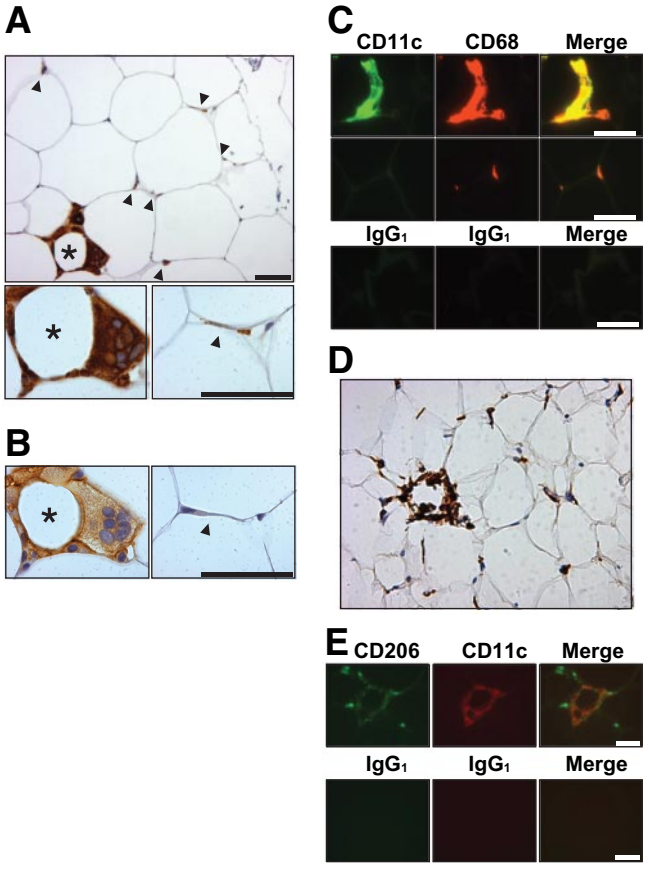

FIG. 1. Immunohistochemistry of subcutaneous adipose tissue in obesity. *A*: Formalin-fixed adipose tissue section stained for CD68 showing a crown (*) and several resident ATMs (arrowheads). *B*: Serial section stained for CD11c showing crown ATMs preferentially expressing CD11c. *C*: Formalin-fixed adipose section stained for CD11c and CD68 or with nonspecific isotype control antibodies confirming that crown ATMs (*upper panel*) but not resident ATMs (*middle panel*) express CD11c. *D*: Frozen adipose tissue section stained for CD206 showing a crown (*) and several resident ATMs. *E*: Frozen section stained for CD206 and CD11c (*upper panel*) or with isotype control antibodies (*lower panel*) showing crown ATMs expressing both CD11c and CD206 but resident ATMs expressing only CD206. Scale bar in all images = 50 μm. (A high-quality digital representation of this figure is available in the online issue.)

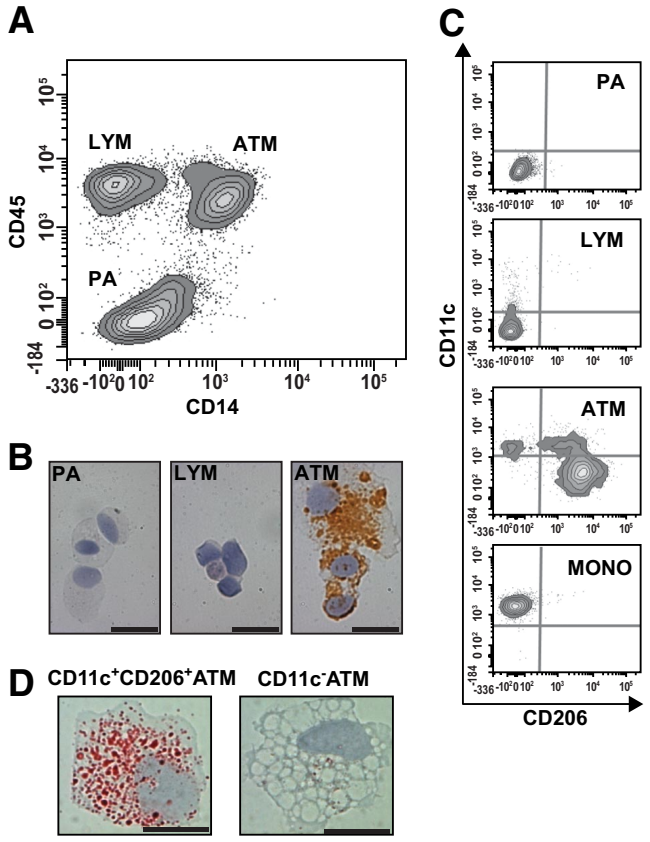

FIG. 2. Flow cytometry of subcutaneous adipose tissue stromovascular cells. *A*: After excluding doublets and dead cells, a CD14 versus CD45 contour plot identified three stromovascular cell populations (PAs, LYMs, and ATMs). *B*: Cytospins of each population stained for CD68 confirmed that the $CD14^+CD45^+$ population represents ATMs. Scale bar = 20 μm. *C*: Flow cytometry phenotype of gated PA, LYM and ATM populations stained for CD11c and CD206 reveals that PA cells do not express either marker, while a minority of LYM cells express low levels of CD11c. ATM cells could be separated into three distinct subpopulations when stained for CD11c and CD206; one of these, $CD11c^+CD206^-$ ATMs, had a similar phenotype to blood monocytes (MONO). Background staining by isotype control antibodies is indicated by gray lines. *D*: $CD11c^+CD206^-$ and $CD11c^-$ ATMs were isolated by flow cytometry cell sorting and stained with Oil red O. Representative images show $CD11c^+CD206^+$ ATMs contain more lipid than $CD11c^-$ ATMs. Scale bar = 10 μm. (A high-quality digital representation of this figure is available in the online issue.)

and venules, and, infrequently, in omental adipose tissue lymphoid aggregates. Serial sections were stained for CD11c, a marker of mouse proinflammatory ATMs (6). CD11c was predominantly expressed by crown ATMs, although many resident ATMs showed weak CD11c staining (Fig. 1*B*). Preferential expression of CD11c by crown ATMs was confirmed by fluorescence microscopy (Fig. 1*C*). CD11c immunoreactivity was exclusive to $CD68^+$ cells. Sections were also stained for CD206, a marker of ATMs that does not stain monocytes (21). By light microscopy, CD206 staining intensity was similar in resident and crown ATMs (Fig. 1*D*), but by fluorescence microscopy staining was weaker in crown ATMs (Fig. 1*E*).

Analysis of crown and resident ATMs by flow cytometry. To analyze ATMs in more detail, flow cytometry was performed on stromovascular cells isolated from digested subcutaneous and omental adipose tissue. Because CD68 is an intracellular antigen, anti-CD14 and -CD45 antibodies were used to identify ATMs, PAs (23), and $CD14^-CD45^+$ cells; the latter were designated LYM because most also expressed the T-cell marker, CD3 (Fig. 2*A*). By immunohistochemistry (Fig. 2*B*), CD68 expression was specific to ATMs. We determined the phenotypes of stromovascular cells with antibodies to CD11c and CD206 (Fig. 2*C*). CD206 was expressed by all $CD11c^-$ ATMs and not by PAs or LYM. However, only a subset of $CD11c^+$ ATMs expressed CD206. As with fluorescence microscopy (Fig. 1*E*), these $CD11c^+$ ATMs had a lower CD206 fluorescence intensity than $CD11c^-$ ATMs. In addition, staining with Oil red O revealed that they contained more intracellular lipid than $CD11c^-$ ATMs (Fig. 2*D*). $CD11c^+CD206^-$ ATMs had a similar profile to blood monocytes (Fig. 2*C*). Together with immunohistochemistry, flow cytometry demonstrated that $CD11c^-$, $CD11c^+CD206^+$, and $CD11c^+CD206^-$ ATM populations represent, respectively, resident ATMs, crown ATMs, and adipose tissue monocytes. While $CD11c^+CD206^-$ cells were rarely observed in adipose tissue sections (Fig. 1*E*), they were readily detected by flow cytometry (Fig. 2*C*). In addition, due to the presence of lymphoid aggregates, omental samples sometimes contained very high numbers of LYM cells and $CD11c^+CD206^-$ ATMs.

TABLE 1
Clinical characteristics of the FOb, Ob, and ObMS women studied*

	FOb (n = 5)			
	Obese	Lean	Ob (n = 12)	ObMS (n = 12)
Age (years)	35 ± 5 (20–52)	39 ± 6 (21–54)†	46 ± 2 (28–55)	47 ± 3 (30–61)†
BMI (kg/m^2)	40 ± 3 (34–46)	26 ± 1 (23–30)‡	46 ± 1 (39–53)	44 ± 1 (39–56)
Waist-to-hip ratio	0.85 ± 0.01 (0.82–0.87)	0.80 ± 0.01 (0.76–0.82)‡	0.85 ± 0.02 (0.75–0.98)	0.93 ± 0.02 (0.86–1.1)‡§
Fasting glucose (mmol/l)	4.6 ± 0.3 (3.8–5.5)	4.5 ± 0.2 (4.1–5.0)	5.0 ± 0.1 (4.7–5.5)	6.4 ± 0.5 (5.0–10.0)†§
Fasting insulin (mIU/l)	12 ± 1 (8–15)	4 ± 0.4 (3–5)‡	13 ± 2 (4–26)	24 ± 3 (13–47)§
HOMA-IR	1.5 ± 0.2 (1.0–2.0)	0.46 ± 0.05 (0.4–0.6)‡	1.6 ± 0.3 (0.5–3.3)	3.2 ± 0.4 (1.7–6.3)‡§
Fasting triglycerides (mmol/l)	1.4 ± 0.3 (0.8–2.5)	1.0 ± 0.2 (0.7–1.7)	1.4 ± 0.1 (0.6–2.5)	2.4 ± 0.4 (1.1–6.2)†‖
HDL (mmol/l)	1.5 ± 0.1 (1.4–1.7)	1.4 ± 0.1 (1.1–1.7)	1.5 ± 0.1 (1.2–2.0)	1.1 ± 0.1 (0.7–1.7)†‖
Alanine transaminase (IU/l)	25 ± 7 (12–53)	17 ± 2 (14–22)	20 ± 2 (14–35)	44 ± 10 (16–144)§
Hypertension	1/5	1/5	2/12	5/9
Type 2 diabetes	0/5	0/5	0/12	3/12
Metabolic syndrome score	1.4 ± 0.2 (1–2)	0.2 ± 0.2 (0–1)‡	1.3 ± 0.5 (1–2)	3.4 ± 0.7 (3–5)‡§
Fasting adiponectin (mg/l)	NP	19 ± 3 (11–26)	13 ± 1 (8–25)	11 ± 1 (7–22)
Fasting HMW adiponectin (mg/l)	NP	15 ± 3 (7–25)	9 ± 1 (5–21)	7 ± 1 (4–15)
Fasting leptin (mg/l)	NP	47 ± 5 (35–61)	64 ± 7 (34–100)	65 ± 9 (34–130)

Continuous data are means ± SE (range). *Metabolic syndrome is defined as three or more of the following: waist >88 cm, blood pressure >130/85 mmHg, fasting glucose >5.6 mmol/l, HDL <1.2 mmol/l, and triglycerides >1.7 mmol/l. †$P < 0.05$ cf obese FOb; ‡$P < 0.005$ cf obese FOb; §$P < 0.005$ cf Ob; ‖$P < 0.05$ cf Ob. NP, not performed.

Crown ATMs are markers of insulin resistance. To determine the relationship between ATM populations and insulin resistance, ATM density was quantitated in subcutaneous and omental adipose tissue from three groups of women: formerly obese (FOb), obese (Ob), and obese with metabolic syndrome (ObMS) (Table 1). The Ob and ObMS groups were comparable in age and BMI, two independent determinants of ATM density in humans (15,17). Histologically, in both adipose tissue depots, crown ATM density was usually zero in FOb and higher in ObMS than Ob (Fig. 3*A*). In addition, in ObMS, crown density was higher in subcutaneous than omental adipose tissue. The differences between Ob and ObMS adipose tissue were not explained by differences in adipocyte size (Fig. 3*B*).

ATM density was then measured by flow cytometry, expressed as percent viable cells within the stromovascular population. None of the omental samples from all 29 women studied contained lymphoid aggregates. Crown density and CD11c$^+$CD206$^+$ ATM density were significantly correlated (Fig. 3*C*), validating flow cytometric assessment. In both subcutaneous and omental adipose tissue, obesity was associated with a significant increase in densities of CD11c$^+$CD206$^-$ (monocyte) (not shown), CD11c$^+$CD206$^+$ (crown) (Fig. 3*D*), and CD11c$^-$ (resident) (Fig. 3*E*) ATMs. Insulin resistance was associated with increased numbers of CD11c$^+$CD206$^+$ ATMs (Fig. 3*D*) but similar numbers of CD11c$^-$ ATMs (Fig. 3*E*). Accordingly, the CD11c$^+$CD206$^+$/CD11c$^-$ ATM ratio was greater in ObMS compared with Ob subjects (Fig. 3*F*). Although the differences in subcutaneous and omental ATM densities between FOb, Ob, and ObMS were qualitatively similar, crown and CD11c$^+$CD206$^+$ ATM densities were lower in omental adipose tissue. LYM and PA densities were increased and decreased, respectively, in obesity but were not significantly different between Ob and ObMS (not shown).

In the 24 obese women, the CD11c$^+$CD206$^+$/CD11c$^-$ ATM ratio correlated significantly with insulin resistance (HOMA of insulin resistance [HOMA-IR]) (Fig. 3*G*). In contrast, there was no correlation between HOMA-IR and CD11c$^-$ ATM density, age, or BMI. A similar and more significant correlation between the HOMA-IR and CD11c$^+$CD206$^+$/CD11c$^-$ ATM ratio was confirmed in another 89 obese women, particularly in subcutaneous adipose tissue (Fig. 3*H*). These results, together with the comparison of ATM densities between the Ob and ObMS above, implicate CD11c$^+$CD206$^+$ ATMs in the pathogenesis of insulin resistance.

Crown ATMs have an M1 surface phenotype. To further characterize ATMs, cell surface marker expression was determined by flow cytometry. Results were similar for subcutaneous and omental ATMs and are shown therefore only for subcutaneous ATMs and blood monocytes (Fig. 4). Expression of the innate immune molecules CD14, Toll-like receptor (TLR)2, TLR4, and C-C receptor (CCR)2 was highest on blood monocytes, with variable expression by ATM subtypes. Expression of integrins was highest on blood monocytes and progressively declined from CD11c$^+$CD206$^-$ to CD11c$^+$CD206$^+$ to CD11c$^-$ ATMs. In contrast, CD11c$^-$ ATMs expressed the highest levels of CD163, a marker of alternative macrophage activation (24), and CD34, a marker of adipogenic/angiogenic ATMs (7). Finally, CD11c$^+$CD206$^+$ ATMs expressed the highest levels of CD45, the antigen-presenting molecules CD1c and HLA-DR, and the T-cell costimulatory molecule CD86. This was most striking for CD1c, which is known to bind and present lipid antigens.

Crown ATMs are the major source of proinflammatory cytokines and chemokines. To determine their potential contribution to adipose tissue inflammation, stromovascular cells were isolated and cultured overnight, and secreted cytokines and chemokines were measured in

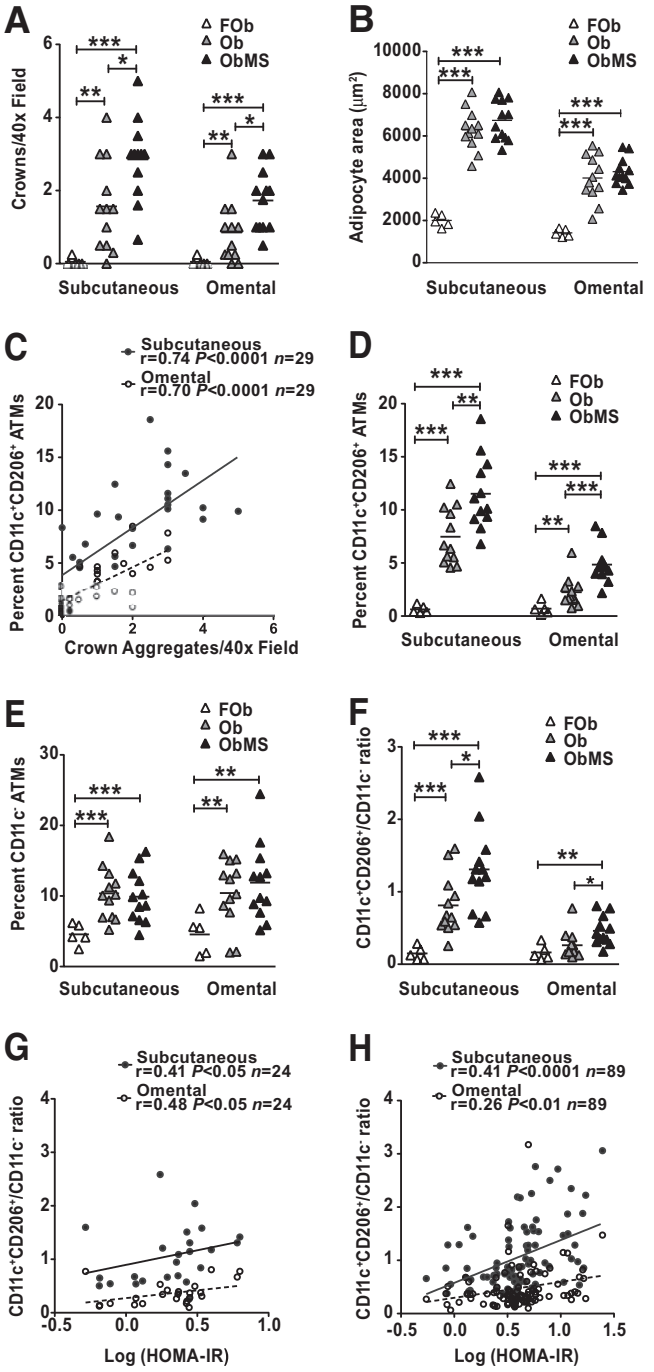

FIG. 3. ***A*** **and** ***B*****: ATM quantitation in subcutaneous and omental adipose obtained from FOb, Ob, and ObMS women. Crown density and mean adipocyte size determined by histology.** ***C*****: Significant correlation between histological and flow cytometry measures of crown ATM density.** ***D*** **and** ***E*****: CD11c$^+$CD206$^+$ (crown) and CD11c$^-$ (resident) ATM densities determined by flow cytometry.** ***F*****: The CD11c$^+$CD206$^+$/CD11c$^-$ ratio is increased in ObMS women, confirming enrichment of crown ATMs in the metabolic syndrome.** ***G*** **and** ***H*****: Relationship between insulin resistance and CD11c$^+$CD206$^+$/CD11c$^-$ ratio in subcutaneous and omental adipose in the initial cohort of 24 obese women and in a subsequent cohort of 89 obese women. *, **, ***$P < 0.05$, 0.005, 0.0005, respectively (Mann Whitney *t* test).**

conditioned medium. Insufficient CD11c$^+$CD206$^-$ adipose tissue monocytes could be isolated for these experiments. ATMs from subcutaneous adipose tissue of three different donors secreted at least 50-fold–higher amounts of IL-1β, IL-6, IL-8, IL-10, tumor necrosis factor (TNF)-α, and CCL3 compared with PA and LYM populations. In each donor, comparison of the two ATM subtypes revealed that unstimulated CD11c$^+$CD206$^+$ ATMs secreted more IL-1β, IL-6, IL-8, IL-10, TNF-α, and CCL3 than CD11c$^-$ ATMs, with IL-8 most highly and IL-10 most differentially secreted (Fig. 5). LPS induced a nonselective increase in cytokine/chemokine secretion by both ATM subtypes. No clear differences in cytokine/chemokine secretion were detected between subcutaneous and omental ATMs (data not shown).

Crown ATMs are enriched for mitochondria and T-cell chemoattractants. CD11c$^+$CD206$^+$ and CD11c$^-$ ATM transcriptomes were compared by microarray. RNA was prepared from subcutaneous ATMs isolated from six obese women. A total of 3,825 differentially expressed genes were identified at a false discovery rate of 5% (supplemental Table 1). Genes encoding CD1c, CD11a, CD11c, CD49d, CD86, CD163, and HLA-DR were differentially expressed in a pattern consistent with the flow cytometry findings. In addition, differential expression of CD11c (*ITGAX*), the fatty acid metabolism genes *APOE* and *FABP4*, and the collagen genes *COL1A2* and *COL6A3* was validated by RT-PCR in independently prepared ATMs (supplemental Fig. 1).

Functional annotation clustering analysis (25), comparing the 1,756 genes upregulated in CD11c$^+$CD206$^+$ ATMs to all human genes, revealed a striking enrichment for genes encoding mitochondrial proteins. It was then demonstrated that CD11c$^+$CD206$^+$ ATMs contain greater numbers of mitochondria, by immunohistochemical staining for the mitochondrial VDAC1 (Fig. 6*A*) and by determining mitochondrial DNA copy number in sorted stromovascular cell populations (Fig. 6*B*). Staining with Mitotracker red demonstrated that CD11c$^+$CD206$^+$ ATMs, together with PAs, have the highest mitochondrial activity within the stromovascular population (Fig. 6*C*). Clustering analysis also revealed that CD11c$^+$CD206$^+$ ATMs were enriched for transcripts encoding glucose and fatty acid metabolism proteins, integrins, proteosomal and lysosomal proteins, and T-cell activation proteins. In contrast, of 2,069 genes upregulated in CD11c$^-$ ATMs, scavenger receptors, the transforming growth factor-β family of cytokines, components of the extracellular matrix, and platelet-derived growth factor-β were overrepresented.

Crown ATM-conditioned medium inhibits insulin action. To determine whether products of ATMs could inhibit insulin action, insulin-stimulated glucose uptake by human SGBS adipocytes was measured in the presence of 20% vol/vol serum-free medium conditioned by stromovascular cells or flow-sorted CD11c$^+$CD206$^+$ ATMs, CD11c$^-$ ATMs, LYM, or PA cells. In four independent experiments, medium conditioned by CD11c$^+$CD206$^+$ crown ATMs consistently inhibited glucose uptake at 1 and 10 nmol/l insulin (Fig. 7).

DISCUSSION

This study documents, for the first time, two ATM subsets in human obesity with distinct anatomical and functional properties. CD11c$^+$CD206$^+$ ATMs localize to crowns and express higher levels of integrins, antigen presentation molecules, and proinflammatory cytokines and one or more secreted factors that impair insulin action. These are features of classically activated macrophages (24,26), yet CD11c$^+$CD206$^+$ ATMs also have features of alternatively activated macrophages, namely high mitochondrial copy

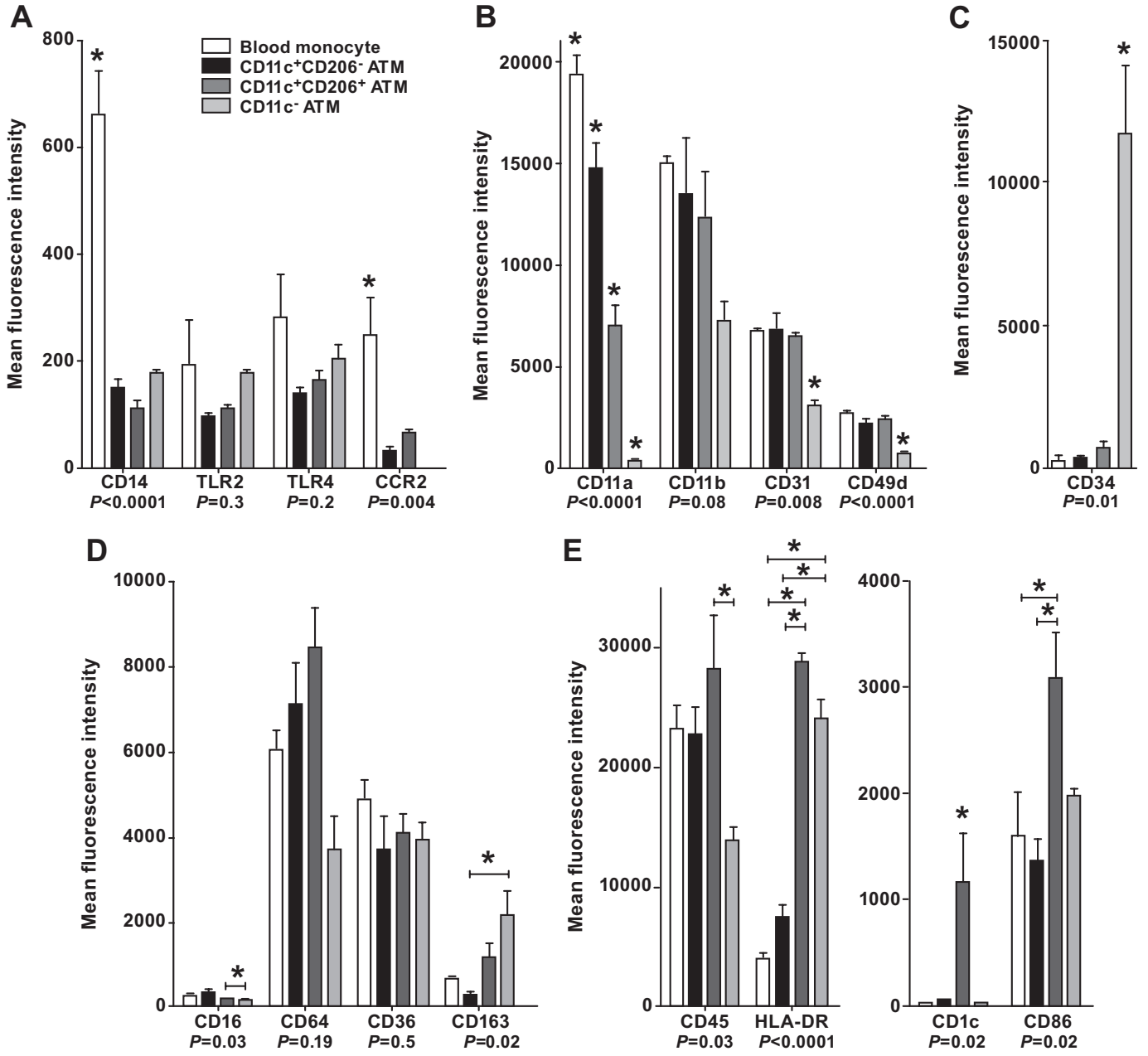

FIG. 4. *A*: Cell surface phenotype of subcutaneous ATMs and blood monocytes. Innate immune molecules. *B*: Integrins. *C*: CD34. *D*: Scavenger receptors. *E*: Adaptive immune molecules. Monocytes and ATM subsets were identified using anti-CD206FITC, -CD11c-allophycocyanin, and -CD14PC7 antibodies. PE-conjugated antibodies were used to determine the expression of cell surface markers. Results are means ± SE of three independent experiments. *Significantly different ($P < 0.05$) in ANOVA by posttest comparison.

number (27) and high levels of IL-10 mRNA and protein, both basally and in response to LPS (24,28). $CD11c^-$ ATMs, on the other hand, occur as solitary cells and express high levels of scavenger receptors and genes implicated in tissue maintenance and repair. These are features of alternatively activated macrophages (24). $CD11c^-$ ATMs also express higher levels of CD34, a marker of ATMs within angiogenic cell clusters (7), as well as platelet-derived growth factor-β, a putative mitogen for adipocyte stem cells (29), implying a role for $CD11c^-$ ATMs in adipogenesis. Thus, the M1/M2 paradigm of mouse $CD11c^+/CD11c^-$ ATMs (6) may not be entirely applicable to humans, as previously suggested (21). Causality is virtually impossible to establish in humans but, by analogy with mice in which $CD11c^+$ macrophages or key macrophage genes have been targeted (3–5,11), proinflammatory ATMs may have a primary role in mediating insulin resistance. This is supported by the relationship between the $CD11c^+CD206^+/CD11c^-$ ATM ratio and insulin resistance, the overall proinflammatory profile of $CD11c^+CD206^+$ ATMs, and their ability to impair insulin action in our studies. $CD11c^+CD206^+$ ATMs and/or cells with which they could interact, such as T-cells, may release specific factor(s) that act locally in adipose tissue and/or systemically in key target organs such as liver, muscle, and pancreas.

In age- and BMI-matched obese women, insulin resistance was associated with an increased $CD11c^+CD206^+$ ATM density and $CD11c^+CD206^+/CD11c^-$ ATM ratio; in

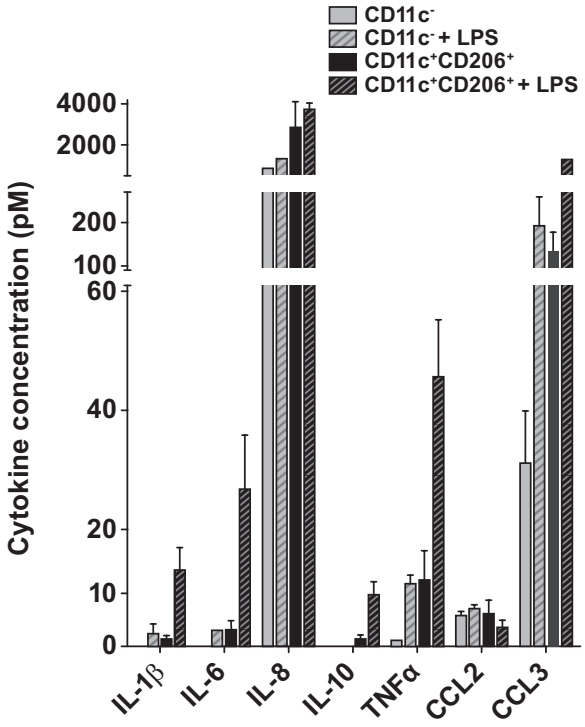

FIG. 5. Cytokine secretion by cultured ATMs subcutaneous CD11c$^-$ and CD11c$^+$CD206$^+$ ATMs (20,000 cells/well) were isolated by flow cytometry cell sorting and cultured in duplicate for 24 h in 100 μl RPMI/10% FCS ± 20 ng/ml LPS. Cytokine concentrations in the supernatant are shown. Results are means ± SE of three independent experiments. Differences between CD11c$^-$ and CD11c$^+$CD206$^+$ ATMs for all cytokines except CCL2 were significant ($P < 0.05$ by paired t test) following normalization.

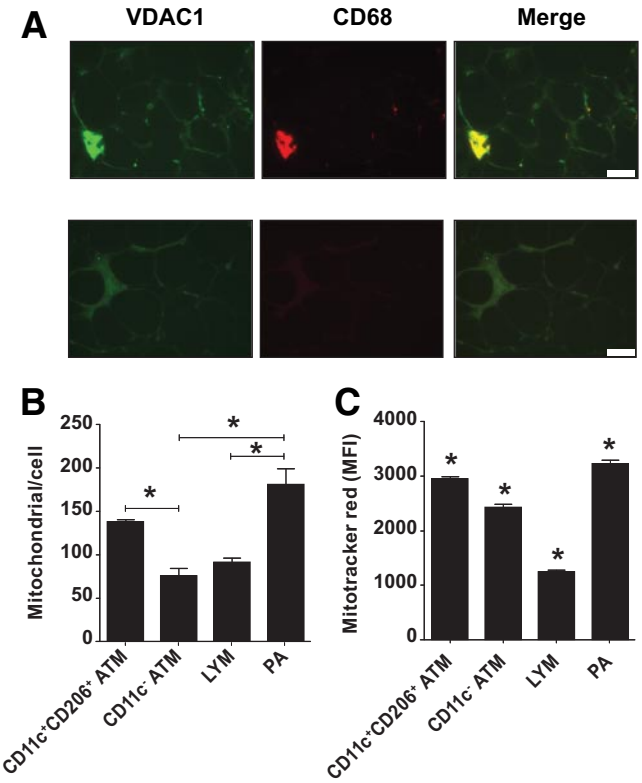

FIG. 6. *A*: Crown ATMs and PAs are enriched for mitochondria. Formalin-fixed adipose section stained with antibodies against VDAC1 and CD68 or nonspecific antibodies. VDAC1 staining intensity was greatest for crown ATMs and less intense for resident ATMs and CD68-negative cells. Scale bar = 50 μm. *B*: Mitochondria per cell was calculated as the relative amount of mitochondrial versus genomic DNA, determined by qPCR of DNA isolated from sorted stromovascular cells using CYTB and LEP primers. Results are means ± SE of three independent experiments. *Significantly different ($P < 0.05$) in ANOVA by posttest comparison. *C*: Stromovascular cells were incubated in RPMI/10% FCS with or without 50 nmol/l Mitotracker red for 15 min in a 37° water bath and then incubated on ice with CD206FITC, CD11cPE, and CD45PC7 antibodies before analysis using flow cytometry. Results are means ± SE of three independent experiments. *Significantly different ($P < 0.05$) in ANOVA by posttest comparison. (A high-quality digital representation of this figure is available in the online issue.)

contrast, CD11c$^-$ ATM density was similar in subcutaneous and omental adipose tissue. Because CD11c$^+$CD206$^+$ ATMs are a minor ATM subpopulation, it is not surprising that previous studies found no association between total ATM density and insulin resistance after correcting for age, sex, and BMI (12,15–17). Our findings highlight the importance of correcting for clinical heterogeneity and quantitating the CD11c$^+$CD206$^+$ ATM subpopulation and are consistent with a recent report (30) that crown macrophage density in subcutaneous abdominal adipose tissue correlated with insulin resistance in an obese, predominately female population. Crown aggregate and CD11c$^+$CD206$^+$ ATM density was lower in omental than subcutaneous adipose tissue, implying that the latter is an important determinant of insulin resistance, but this is at odds with clinical studies that show that visceral adipose tissue correlates better with insulin resistance (31). However, it is consistent with the greater size of subcutaneous versus omental adipocytes and with a recent study in lean and obese men that found subcutaneous, not visceral, fat mass correlated with insulin resistance (32) and would support the view (33) that visceral adiposity is a consequence rather than a cause of insulin resistance. On the other hand, immunohistochemistry with antibodies to HAM56 and CD40, although semiquantitative, identified a higher crown ATM density in omental adipose tissue of obese men and women (15,34). This difference may be methodological or explained by our exclusive study of women or other differences in the study populations.

The relatively high secretion of IL-8 by CD11c$^+$CD206$^+$ ATMs raises the possibility that CD11c$^+$ ATM–derived IL-8 could promote metabolic complications of obesity, consistent with earlier reports that serum IL-8 is increased in obesity and type 2 diabetes (35,36) and that adipocytes are not the predominant source of adipose tissue–derived IL-8 (37,38). While IL-8 is a potent neutrophil chemoattractant (39), neutrophils were not evident on tissue sections or in stromovascular preparations, suggesting another role for CD11c$^+$ ATM–derived IL-8. Further investigation of IL-8 in human obesity will require specific antagonists, as homologues of human IL-8 and its receptor CXCR1 are absent in mice and rats (39).

Phenotyping of ATMs revealed a progressive decrease in expression of integrins from blood monocytes to CD11c$^+$CD206$^-$, CD11c$^+$CD206$^+$, and CD11c$^-$ ATMs and absent expression of the CCL2 chemokine receptor CCR2 on CD11c$^-$ ATMs. This suggests a developmental pathway from blood monocytes to resident ATMs, in accord with mouse studies reporting that ATMs are derived mostly from blood (10,13,14) and that blockade of monocyte recruitment to adipose tissue with a CCL2 receptor antagonist (40) or by genetic ablation of CD49d (41) protects mice against metabolic complications of obesity. Our findings indicate that, in addition to CCR2 antagonists,

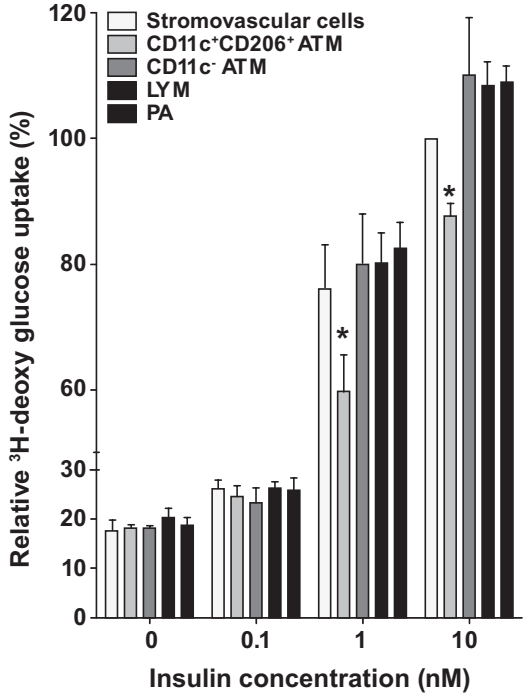

FIG. 7. Crown ATMs release factors that inhibit insulin action serum-free F3 medium was conditioned for 48 h with 50,000 total stromovascular cells, CD11c$^+$CD206$^+$ ATMs, CD11c$^-$ ATM, LYM, or PA cells. Differentiated human SGBS adipocytes were then incubated in conditioned medium (20% vol/vol) in fresh F3 medium for 48 h, before measurement of insulin-stimulated ^{3}H-deoxyglucose uptake. Data (means ± SE) are from four independent experiments using cells isolated from subcutaneous ($n = 3$) and omental ($n = 1$) adipose tissue from three obese women with metabolic syndrome. Glucose uptake was normalized to the cpm values from total stromovascular cell-conditioned medium and 10 nmol/l insulin (100%). *Significantly different ($P < 0.05$) in ANOVA by posttest comparison.

agents that block the integrins CD11a, CD11b, CD11c, CD31, or CD49d might also be therapeutic in this setting.

By microarray, CD11c$^+$CD206$^+$ ATMs were enriched for lipid-rich vacuolar and mitochondrial RNAs and transcripts encoding the lipid-binding proteins APOE and FABP4 and enzymes for fatty acid metabolism. This profile is consistent with a role for CD11c$^+$CD206$^+$ ATMs in converting potentially toxic lipid from dead adipocytes into nontoxic lipoproteins for disposal from adipose tissue into the circulation (8). CD11c$^+$CD206$^+$ ATMs were also enriched for transcripts encoding components of the lysosome and proteasome and for proteins implicated in T-cell attraction and activation. These features, together with their proinflammatory phenotype, raise the possibility that CD11c$^+$CD206$^+$ ATMs could initiate adaptive immune responses to adipose tissue antigens, analogous to presentation of oxidized LDL to T-cells by CD1 on foamy macrophages in atherosclerotic lesions (42). Recent studies (43–45) in obese mice implicate antigen-specific adipose tissue T-cells in insulin resistance and suggest that cross-talk between T-cells and CD11c$^+$CD206$^+$ ATMs could promote insulin resistance and perhaps other complications of obesity in humans. Of the few genes definitely associated with insulin resistance in obesity identified from genome-wide scans, peroxisome proliferator–activated receptor-γ was the only one overrepresented in CD11c$^+$CD206$^+$ ATMs.

In summary, we characterize distinct CD11c$^-$ and CD11c$^+$ subsets of human ATMs and present evidence that CD11c$^+$CD206$^+$ ATMs form crowns, are enriched in the adipose tissue of insulin-resistant women, are proinflammatory, and impair insulin action. It will be important to determine whether CD11c$^+$CD206$^+$ ATMs are also associated with features of the metabolic syndrome in other ethnic groups and in men, whose ATM density is reported to be higher than that of BMI-matched women (15). Finally, identifying the factors elaborated by CD11c$^+$CD206$^+$ ATMs that impair insulin action may lead to novel anti-inflammatory therapies for the complications of obesity.

ACKNOWLEDGMENTS

This work was funded by program (516700) and infrastructure (361646) grants from the National Health and Medical Research Council of Australia (NHMRC), a Victorian State Government Operational Infrastructure Support Grant, the Diabetes Australia Research Trust, and the Royal Australian College of Physicians Research Foundation.

J.M.W. is a Doherty Fellow and L.C.H. is a Senior Principal Research Fellow of the NHMRC.

No potential conflicts of interest relevant to this article were reported.

We thank the women who participated in this study, the staff of The Avenue Hospital who assisted with adipose tissue collection, and Jennifer Carden and Anthony Burn for blood sampling. Jon Whitehead arranged transfer of SGBS cells to our laboratory, and Catherine McLean provided secretarial assistance.

REFERENCES

1. O'Brien PE, Dixon JB, Laurie C, Skinner S, Proietto J, McNeil J, Strauss B, Marks S, Schachter L, Chapman L, Anderson M. Treatment of mild to moderate obesity with laparoscopic adjustable gastric banding or an intensive medical program: a randomized trial. Ann Intern Med 2006;144:625–633
2. Strissel KJ, Stancheva Z, Miyoshi H, Perfield JW 2nd, DeFuria J, Jick Z, Greenberg AS, Obin MS. Adipocyte death, adipose tissue remodeling, and obesity complications. Diabetes 2007;56:2910–2918
3. Arkan MC, Hevener AL, Greten FR, Maeda S, Li ZW, Long JM, Wynshaw-Boris A, Poli G, Olefsky J, Karin M. IKK-beta links inflammation to obesity-induced insulin resistance. Nat Med 2005;11:191–198
4. Hevener AL, Olefsky JM, Reichart D, Nguyen MT, Bandyopadyhay G, Leung HY, Watt MJ, Benner C, Febbraio MA, Nguyen AK, Folian B, Subramaniam S, Gonzalez FJ, Glass CK, Ricote M. Macrophage PPAR-gamma is required for normal skeletal muscle and hepatic insulin sensitivity and full antidiabetic effects of thiazolidinediones. J Clin Invest 2007;117:1658–1669
5. Odegaard JI, Ricardo-Gonzalez RR, Goforth MH, Morel CR, Subramanian V, Mukundan L, Eagle AR, Vats D, Brombacher F, Ferrante AW, Chawla A. Macrophage-specific PPARgamma controls alternative activation and improves insulin resistance. Nature 2007;447:1116–1120
6. Lumeng CN, Bodzin JL, Saltiel AR. Obesity induces a phenotypic switch in adipose tissue macrophage polarization. J Clin Invest 2007;117:175–184
7. Nishimura S, Manabe I, Nagasaki M, Hosoya Y, Yamashita H, Fujita H, Ohsugi M, Tobe K, Kadowaki T, Nagai R, Sugiura S. Adipogenesis in obesity requires close interplay between differentiating adipocytes, stromal cells, and blood vessels. Diabetes 2007;56:1517–1526
8. Cinti S, Mitchell G, Barbatelli G, Murano I, Ceresi E, Faloia E, Wang S, Fortier M, Greenberg AS, Obin MS. Adipocyte death defines macrophage localization and function in adipose tissue of obese mice and humans. J Lipid Res 2005;46:2347–2355
9. Nguyen MT, Favelyukis S, Nguyen AK, Reichart D, Scott PA, Jenn A, Liu-Bryan R, Glass CK, Neels JG, Olefsky JM. A subpopulation of macrophages infiltrates hypertrophic adipose tissue and is activated by free fatty acids via Toll-like receptors 2 and 4 and JNK-dependent pathways. J Biol Chem 2007;282:35279–35292
10. Lumeng CN, Delproposto JB, Westcott DJ, Saltiel AR. Phenotypic switching of adipose tissue macrophages with obesity is generated by spatiotemporal differences in macrophage subtypes. Diabetes 2008;57:3239–3246
11. Patsouris D, Li PP, Thapar D, Chapman J, Olefsky JM, Neels JG. Ablation of CD11c-positive cells normalizes insulin sensitivity in obese insulin resistant animals. Cell Metab 2008;8:301–309

12. Cancello R, Henegar C, Viguerie N, Taleb S, Poitou C, Rouault C, Coupaye M, Pelloux V, Hugol D, Bouillot JL, Bouloumie A, Barbatelli G, Cinti S, Svensson PA, Barsh GS, Zucker JD, Basdevant A, Langin D, Clement K. Reduction of macrophage infiltration and chemoattractant gene expression changes in white adipose tissue of morbidly obese subjects after surgery-induced weight loss. Diabetes 2005;54:2277–2286
13. Weisberg SP, McCann D, Desai M, Rosenbaum M, Leibel RL, Ferrante AW Jr. Obesity is associated with macrophage accumulation in adipose tissue. J Clin Invest 2003;112:1796–1808
14. Xu H, Barnes GT, Yang Q, Tan G, Yang D, Chou CJ, Sole J, Nichols A, Ross JS, Tartaglia LA, Chen H. Chronic inflammation in fat plays a crucial role in the development of obesity-related insulin resistance. J Clin Invest 2003;112:1821–1830
15. Cancello R, Tordjman J, Poitou C, Guilhem G, Bouillot JL, Hugol D, Coussieu C, Basdevant A, Hen AB, Bedossa P, Guerre-Millo M, Clement K. Increased infiltration of macrophages in omental adipose tissue is associated with marked hepatic lesions in morbid human obesity. Diabetes 2006;55:1554–1561
16. Di Gregorio GB, Yao-Borengasser A, Rasouli N, Varma V, Lu T, Miles LM, Ranganathan G, Peterson CA, McGehee RE, Kern PA. Expression of CD68 and macrophage chemoattractant protein-1 genes in human adipose and muscle tissues: association with cytokine expression, insulin resistance, and reduction by pioglitazone. Diabetes 2005;54:2305–2313
17. Harman-Boehm I, Bluher M, Redel H, Sion-Vardy N, Ovadia S, Avinoach E, Shai I, Kloting N, Stumvoll M, Bashan N, Rudich A. Macrophage infiltration into omental versus subcutaneous fat across different populations: effect of regional adiposity and the comorbidities of obesity. J Clin Endocrinol Metab 2007;92:2240–7
18. McTernan PG, Kusminski CM, Kumar S. Resistin. Curr Opin Lipidol 2006;17:170–175
19. Weinberg JB, Misukonis MA, Shami PJ, Mason SN, Sauls DL, Dittman WA, Wood ER, Smith GK, McDonald B, Bachus KE, et al. Human mononuclear phagocyte inducible nitric oxide synthase (iNOS): analysis of iNOS mRNA, iNOS protein, biopterin, and nitric oxide production by blood monocytes and peritoneal macrophages. Blood 1995;86:1184–1195
20. Schneemann M, Schoeden G. Macrophage biology and immunology: man is not a mouse. J Leukoc Biol 2007;81:579; discussion 580
21. Zeyda M, Farmer D, Todoric J, Aszmann O, Speiser M, Gyori G, Zlabinger GJ, Stulnig TM. Human adipose tissue macrophages are of an anti-inflammatory phenotype but capable of excessive pro-inflammatory mediator production. Int J Obes (Lond) 2007;31:1420–8
22. McLaughlin T, Deng A, Gonzales O, Aillaud M, Yee G, Lamendola C, Abbasi F, Connolly AJ, Sherman A, Cushman SW, Reaven G, Tsao PS. Insulin resistance is associated with a modest increase in inflammation in subcutaneous adipose tissue of moderately obese women. Diabetologia 2008;51:2303–2308
23. Curat CA, Miranville A, Sengenes C, Diehl M, Tonus C, Busse R, Bouloumie A. From blood monocytes to adipose tissue-resident macrophages: induction of diapedesis by human mature adipocytes. Diabetes 2004;53:1285–1292
24. Mantovani A, Sica A, Sozzani S, Allavena P, Vecchi A, Locati M. The chemokine system in diverse forms of macrophage activation and polarization. Trends Immunol 2004;25:677–686
25. Dennis G Jr, Sherman BT, Hosack DA, Yang J, Gao W, Lane HC, Lempicki RA. DAVID: Database for Annotation, Visualization, and Integrated Discovery Genome Biol 2003;4:P3
26. Gordon S, Taylor PR. Monocyte and macrophage heterogeneity. Nat Rev Immunol 2005;5:953–964
27. Vats D, Mukundan L, Odegaard JI, Zhang L, Smith KL, Morel CR, Greaves DR, Murray PJ, Chawla A. Oxidative metabolism and PGC-1beta attenuate macrophage-mediated inflammation. Cell Metab 2006;4:13–24
28. Verreck FA, de Boer T, Langenberg DM, Hoeve MA, Kramer M, Vaisberg E, Kastelein R, Kolk A, de Waal-Malefyt R, Ottenhoff TH. Human IL-23-producing type 1 macrophages promote but IL-10-producing type 2 macrophages subvert immunity to (myco)bacteria. Proc Natl Acad Sci U S A 2004;101:4560–4565
29. Tang W, Zeve D, Suh JM, Bosnakovski D, Kyba M, Hammer RE, Tallquist MD, Graff JM. White fat progenitor cells reside in the adipose vasculature. Science 2008;322:583–586
30. Apovian CM, Bigornia S, Mott M, Meyers MR, Ulloor J, Gagua M, McDonnell M, Hess D, Joseph L, Gokce N. Adipose macrophage infiltration is associated with insulin resistance and vascular endothelial dysfunction in obese subjects. Arterioscler Thromb Vasc Biol 2008;28:1654–1659
31. Lebovitz HE, Banerji MA. Point: visceral adiposity is causally related to insulin resistance. Diabetes Care 2005;28:2322–2325
32. Frederiksen L, Nielsen TL, Wraae K, Hagen C, Frystyk J, Flyvbjerg A, Brixen K, Andersen M. Subcutaneous rather than visceral adipose tissue is associated with adiponectin levels and insulin resistance in young men. J Clin Endocrinol Metab 2009;94:4010–4015
33. Miles JM, Jensen MD. Counterpoint: visceral adiposity is not causally related to insulin resistance. Diabetes Care 2005;28:2326–2328
34. Aron-Wisnewsky J, Tordjman J, Poitou C, Darakhshan F, Hugol D, Basdevant A, Aissat A, Guerre-Millo M, Clement K. Human adipose tissue macrophages: M1 and M2 cell surface markers in subcutaneous and omental depots and after weight loss. J Clin Endocrinol Metab 2009;94:4619–23
35. Bruun JM, Verdich C, Toubro S, Astrup A, Richelsen B. Association between measures of insulin sensitivity and circulating levels of interleukin-8, interleukin-6 and tumor necrosis factor-alpha: effect of weight loss in obese men Eur J Endocrinol 2003;148:535–542
36. Zozulinska D, Majchrzak A, Sobieska M, Wiktorowicz K, Wierusz-Wysocka B. Serum interleukin-8 level is increased in diabetic patients. Diabetologia 1999;42:117–118
37. Bruun JM, Lihn AS, Madan AK, Pedersen SB, Schiott KM, Fain JN, Richelsen B. Higher production of IL-8 in visceral vs. subcutaneous adipose tissue. Implication of nonadipose cells in adipose tissue. Am J Physiol Endocrinol Metab 2004;286:E8–E13
38. Fain JN, Madan AK, Hiler ML, Cheema P, Bahouth SW. Comparison of the release of adipokines by adipose tissue, adipose tissue matrix, and adipocytes from visceral and subcutaneous abdominal adipose tissues of obese humans. Endocrinology 2004;145:2273–2282
39. Remick DG. Interleukin-8. Crit Care Med 2005;33:S466–S467
40. Weisberg SP, Hunter D, Huber R, Lemieux J, Slaymaker S, Vaddi K, Charo I, Leibel RL, Ferrante AW Jr. CCR2 modulates inflammatory and metabolic effects of high-fat feeding. J Clin Invest 2006;116:115–124
41. Feral CC, Neels JG, Kummer C, Slepak M, Olefsky JM, Ginsberg MH. Blockade of alpha4 integrin signaling ameliorates the metabolic consequences of high-fat diet–induced obesity. Diabetes 2008;57:1842–1851
42. Melian A, Geng YJ, Sukhova GK, Libby P, Porcelli SA. CD1 expression in human atherosclerosis: a potential mechanism for T cell activation by foam cells Am J Pathol 1999;155:775–786
43. Feuerer M, Herrero L, Cipolletta D, Naaz A, Wong J, Nayer A, Lee J, Goldfine AB, Benoist C, Shoelson S, Mathis D. Lean, but not obese, fat is enriched for a unique population of regulatory T cells that affect metabolic parameters. Nat Med 2009;15:930–939
44. Nishimura S, Manabe I, Nagasaki M, Eto K, Yamashita H, Ohsugi M, Otsu M, Hara K, Ueki K, Sugiura S, Yoshimura K, Kadowaki T, Nagai R. CD8+ effector T cells contribute to macrophage recruitment and adipose tissue inflammation in obesity. Nat Med 2009;15:914–920
45. Winer S, Chan Y, Paltser G, Truong D, Tsui H, Bahrami J, Dorfman R, Wang Y, Zielenski J, Mastronardi F, Maezawa Y, Drucker DJ, Engleman E, Winer D, Dosch HM. Normalization of obesity-associated insulin resistance through immunotherapy. Nat Med 2009;15:921–929
46. Levy JC, Matthews DR, Hermans MP. Correct homeostasis model assessment (HOMA) evaluation uses the computer program. Diabetes Care 1998;21:2191–2192
47. Fischer-Posovsky P, Newell FS, Wabitsch M, Tornqvist HE. Human SGBS cells: a unique tool for studies of human fat cell biology. Obesity Facts 2008;1:184–189
48. Gentleman RC, Carey VJ, Bates DM, Bolstad B, Dettling M, Dudoit S, Ellis B, Gautier L, Ge Y, Gentry J, Hornik K, Hothorn T, Huber W, Iacus S, Irizarry R, Leisch F, Li C, Maechler M, Rossini AJ, Sawitzki G, Smith C, Smyth G, Tierney L, Yang JY, Zhang J. Bioconductor: open software development for computational biology and bioinformatics. Genome Biol 2004;5:R80
49. Lin SM, Du P, Huber W, Kibbe WA. Model-based variance-stabilizing transformation for Illumina microarray data. Nucleic Acid Res 2008;36:e11
50. Smyth GK. Linear models and empirical bayes methods for assessing differential expression in microarray experiments. Stat Appl Genet Mol Biol 2004;3:Article3